RSC Advances

PAPER

View Article Online
View Journal | View Issue

Open Access Article. Published on 12 January 2017. Downloaded on 11/7/2025 3:24:31 PM.
This article is licensed under a Creative Commons Attribution 3.0 Unported Licence.

Cite this: *RSC Adv.*, 2017, 7, 1809

$CH_3NH_3PbI_3$ perovskite:poly(*N*-vinylcarbazole) blends for broadband optical limiting

Ting Bai,[a] Ningning Dong,[b] Hongxia Cheng,[a] Qing Cheng,[a] Jun Wang*[bc] and Yu Chen*[a]

Received 15th October 2016
Accepted 17th November 2016

DOI: 10.1039/c6ra25276a

www.rsc.org/advances

As one of the most active areas in laser protection, organic/inorganic hybrid functional materials have been expected to play an extremely important role in the field of optical limiting. The optical limiting performance of the $CH_3NH_3PbI_3$ perovskite:poly(*N*-vinylcarbazole) (weight ratio: 1 : 1) blends (hereafter abbreviated as CP) was experimentally studied in DMF and in a poly(methylmethlacrylate) (PMMA) matrix, respectively, using an open aperture Z-scan method. In contrast to the CP dispersed in DMF, which showed no apparent nonlinear optical (NLO) response at both 532 and 1064 nm, after annealing at 200 °C in N_2 for 30 min, a saturable absorption (SA) response was observed in the same DMF dispersion under the excitation of 532 nm laser. At 1064 nm, the annealed sample displayed different NLO responses: SA at the lower pulse energy and reverse saturable absorption (RSA) at the higher pulse energy. Both the 3 wt% and 6 wt% CP-doped PMMA composite films exhibited a typical RSA response, larger nonlinear absorption coefficient and superior optical limiting performance when compared to the same blends in DMF dispersion.

In the past decades, significant research effort has been invested in state-of-the-art optical limiting (OL) materials (*e.g.* fullerenes, carbon nanotubes, polymer/nanotube composites, porphyrins, phthalocyanines, mixed metal complexes, carbon black suspensions, two dimensional nanosheets, nanowires, nanofibers and nanoparticles as well) in an attempt to achieve some measure of protection from laser beams.[1–5] A large number of essential strategies have been employed to control and optimize the OL characteristics of nonlinear optical (NLO) materials for practical laser protection. However, the preparation of novel nonlinear and optically active materials with excellent thermal stability, small limiting threshold value, large laser damage threshold value, ps/ns response time and broadband spectral range, still presents a significant challenge.

Since 2009, organometal halide perovskites (*e.g.* $CH_3NH_3MX_3$ (M = Pb, Sn; X = Cl, Br, I), $CH_3NH_3MBr_xX_{(3-x)}$ (M = Pb, Sn; X = Cl, I), $(C_4H_9NH_3)_2(CH_3NH_3)_{(x-1)}Sn_xI_{(3x+1)}$, $CH_3NH_3PbCl_xI_{(3-x)}$ and others) have attracted significant attention worldwide,[6–9] especially in organic photovoltaics (including dye-sensitized solar cells and other organic solar cells), due to their high electron mobility (66–2300 $cm^2\ V^{-1}\ s^{-1}$),[10] long exciton diffusion length (100–1000 nm),[11,12] high linear absorption coefficient ($1.5 \times 10^4\ cm^{-1}$ at 550 nm),[13] tunable bandgap (1.17–2.3 eV).[8,13,14] However, the NLO and OL performances of these materials have been less studied so far.

In this work, we reported for the first time the NLO and OL properties of the $CH_3NH_3PBI_3$ perovskite:poly(*N*-vinylcarbazole) (weight ratio: 1 : 1) blends (CP) in DMF and in the PMMA matrix, respectively, by open aperture Z-scan method. The $CH_3NH_3PbI_3$ perovskite was prepared according to the method described in the literature.[6] Poly(*N*-vinylcarbazole) (PVK, $M_w = 9 \times 10^4$), which processes excellent hole-transporting ability and photoconductivity,[15–17] was chose as electron-donating material to construct the $CH_3NH_3PBI_3$-based donor–acceptor system for nonlinear optics. The energy difference in LUMO levels between PVK (−2.2 eV) and $CH_3NH_3PbI_3$ (−3.9 eV) reached up to 1.7 eV, far more than 0.3 eV,[18] which is a key parameter for realizing 100% charge transfer between electron donor and acceptor.

Both the PVK and $CH_3NH_3PbI_3$ have very good thermal stability. Their onset temperatures for thermal bond cleavage were 480 °C for PVK and 334 °C for $CH_3NH_3PbI_3$, respectively. From Fig. 1a and b, it can be seen that the $CH_3NH_3PbI_3$ crystals achieved in this study have a narrow size distribution in the range of 2–18 nm, with an average diameter of 7.94 nm. The characteristic diffraction peaks of $CH_3NH_3PbI_3$ (Fig. 1c) were found to be centred at $2\theta = 14.1°$ (110), 20.0° (112), 23.6° (211), 24.5° (202), 28.4° (220), 32.0° (310) and 35.0° (312), suggesting typical tetragonal perovskite structure.[19,20] The corresponding crystal faces are indicated in parentheses. The X-ray diffraction (XRD) pattern of PVK had a strong diffraction peak at $2\theta = 7.67°$, from which the nearest chain-to-chain distance was calculated

[a]*Key Laboratory for Advanced Materials, Institute of Applied Chemistry, East China University of Science and Technology, 130 Meilong Road, Shanghai 200237, China. E-mail: chentangyu@yahoo.com*

[b]*Key Laboratory of Materials for High-Power Laser, Shanghai Institute of Optics and Fine Mechanics, CAS, Shanghai 201800, China. E-mail: jwang@siom.ac.cn*

[c]*State Key Laboratory of High Field Laser Physics Shanghai Institute of Optics and Fine Mechanics Chinese Academy of Sciences, Shanghai 201800, China*

Open Access Article. Published on 12 January 2017. Downloaded on 11/7/2025 3:24:31 PM.
This article is licensed under a Creative Commons Attribution 3.0 Unported Licence.

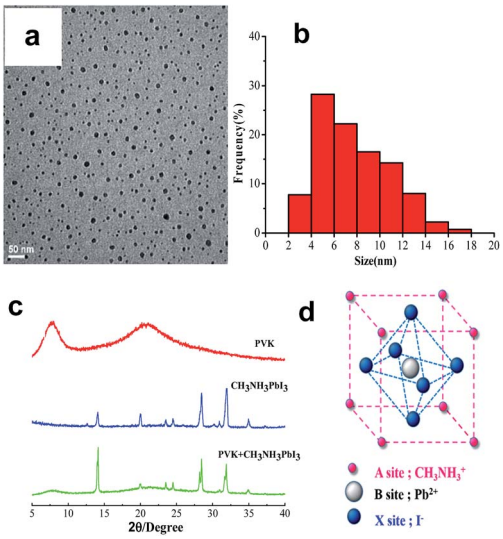

Fig. 1 (a) TEM image and (b) size distribution of the as-prepared $CH_3NH_3PbI_3$, (c) XRD patterns of the film samples, and (d) structural representation of $CH_3NH_3PbI_3$.

to be 11.51 Å, and a broad, diffuse amorphous halo at $2\theta = 20.64°$ ($d = 4.30$ Å). As expected, the XRD pattern of $CH_3NH_3PbI_3$/PVK blends was a simple superposition of the XRD patterns of these two components. No additional information is available.

The NLO and OL properties of CP were experimentally studied in DMF and in the PMMA matrix, respectively, by open aperture Z scan method that was widely used to test the NLO responses of materials. The Z-scan measurements were performed using 6 ns pulses from a Q-switched Nd : YAG laser operating at 1064 and 532 nm. The incident laser was tightly focused with a 15 cm focus lens. All dispersions were tested in 10 × 1 mm quartz cuvettes with the pulse repetition rate of 10 Hz. For the PMMA films, the pulse repetition rate used was 2 Hz. Fig. 2 gives the excitation pulse energy dependent Z-scan data of CP dispersed in DMF before and after annealing at 200 °C in N_2. As seen in Fig. 2a and b, the dispersions show no apparent NLO response before annealing at both 532 and 1064 nm. After annealing for 30 min, a symmetric peak at the beam focus shows up and strengthens gradually with the incident pulse energy increasing at 532 nm, suggesting a saturable absorption (SA) response (Fig. 2c). It is noteworthy that, whatever the sample is PVK or $CH_3NH_3PbI_3$, these materials themselves do not exhibit any NLO effect. At 1064 nm, the annealed sample displays different NLO responses (Fig. 2d). The normalized transmission curve shows a peak at the lowest pulse energy of 250 μJ, which can be assigned to SA. However, as the pulse energy clamping, a valley inside the peak appears at the beam focus and deepens gradually due to the reverse saturable absorption (RSA) mechanism that occurs following SA. These results demonstrated that the annealing treatment on the blends considerably improved the NLO effect of material. A reasonable explanation for this issue is that the annealing treatment on the blends induces more efficient intermolecular charge transfer effect between PVK and $CH_3NH_3PbI_3$ during the annealing process, and consequently further improves the NLO performance of the blends.

To evaluate the NLO performance of CP in the solid state, we embedded it as inclusions in a transparent PMMA matrix. The achieved composite materials with different CP concentrations (3 wt%, 6 wt%) can be directly used to produce suitable solid films for the broadband solid-state OL applications. In comparison with the non-annealed films, the NLO performance of the annealed films experiences a significant improvement.

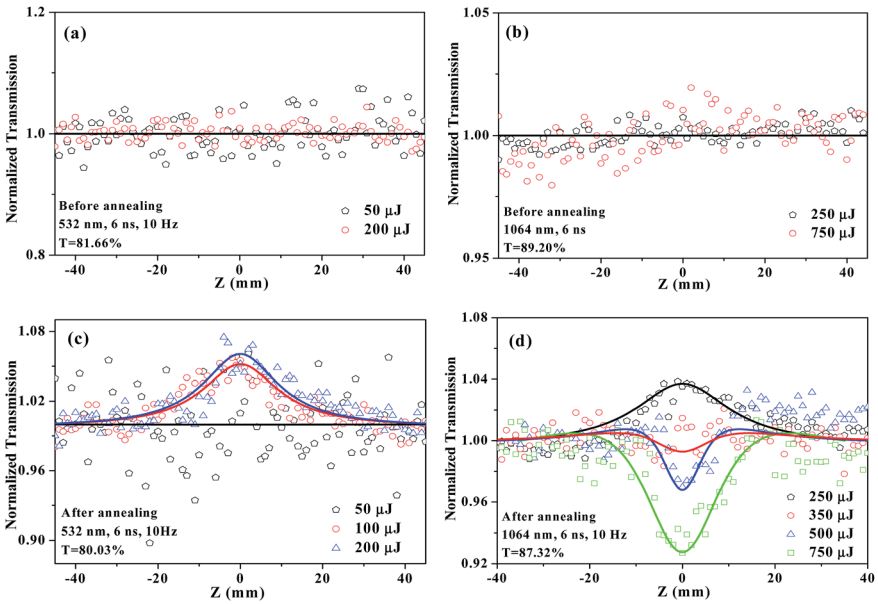

Fig. 2 Normalized open-aperture Z-scan results of the $CH_3NH_3PbI_3$:PVK blends dispersed in DMF before (a, b) and after (c, d) annealing of the blends at 200 °C in N_2 for 30 min, under the excitation of 6 ns pulses at 532 nm (a, c) and 1064 nm (b, d) with different pulse energies. The solid lines are the theoretical fitting results.

Open Access Article. Published on 12 January 2017. Downloaded on 11/7/2025 3:24:31 PM.
This article is licensed under a Creative Commons Attribution 3.0 Unported Licence.

Taking the 3 wt% CP-doped PMMA film, the normalized transmission curve before annealing shows no obvious variation at the lowest pulse energy of 75 μJ at 532 nm, whereas the corresponding curve possesses a valley with the value of ~0.87 in the annealed film (Fig. 3a and c). At 250 μJ, the minimal value of normalized transmittance (T_{min}), which can be used to evaluate the OL response of the materials, is ~0.45 in the annealed film. This value is less than the T_{min} value (~0.65) observed in the non-annealed film. Similar phenomena can also be observed under 1064 nm laser excitation. In contrast to 3 wt% CP-doped PMMA film, the 6 wt% CP-doped film exhibits more superior broadband OL performance before and after annealing due to the higher CP doping level in the resultant film.

To further understand the NLO and OL behaviors of the above films, the normalized transmittances were plotted as functions of incident laser intensity (Fig. 4a and b). As expected, the PMMA film with higher CP concentration shows greater OL performance than that with lower concentration at both 532 and 1064 nm. The T_{min} values were found to be ~0.3 at the excitation intensity of ~1.3 GW cm^{-2} at 532 nm, and ~0.4 at the excitation intensity of ~1.4 GW cm^{-2} at 1064 nm, respectively. Furthermore, the annealed film produces more superior OL response, which is consistent with the results shown in Fig. 3.

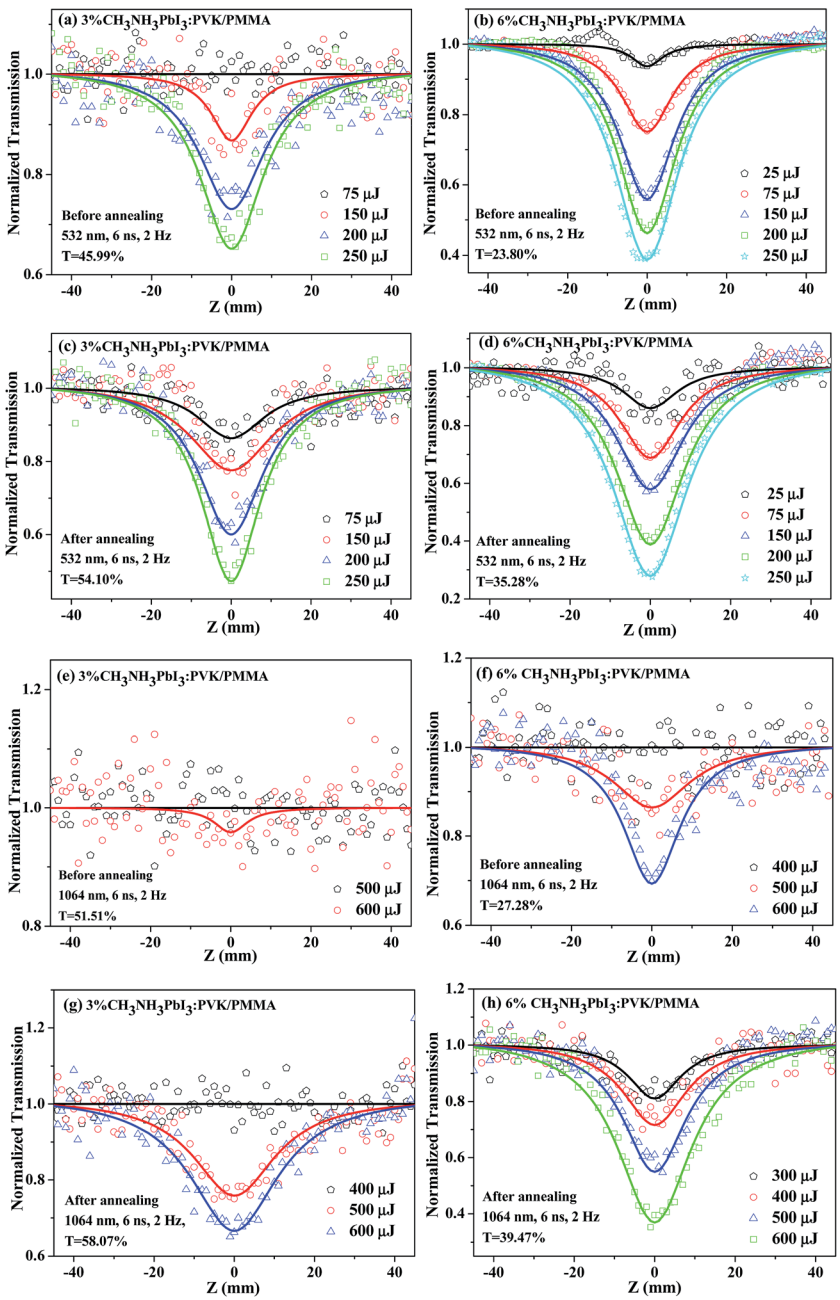

Fig. 3 Typical open-aperture Z-scan data of the $CH_3NH_3PbI_3$:PVK/PMMA films with different $CH_3NH_3PbI_3$:PVK concentrations. The annealing condition: 200 °C for 30 min in N_2.

Open Access Article. Published on 12 January 2017. Downloaded on 11/7/2025 3:24:31 PM.
This article is licensed under a Creative Commons Attribution 3.0 Unported Licence.

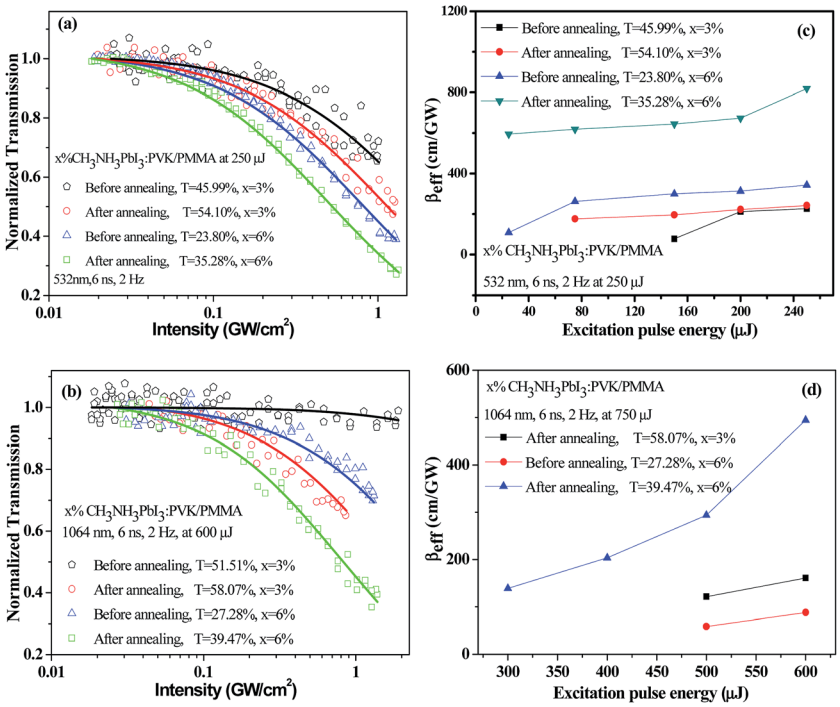

Fig. 4 Variation in the normalized transmittance as a function of input laser intensity and β_{eff} as a function of the excitation pulse energy for the $CH_3NH_3PbI_3$:PVK/PMMA films at 532 nm (a, c) and 1064 nm (b, d), respectively.

Table 1 Linear and NLO data of the samples. CP: $CH_3NH_3PbI_3$:PVK; T_0: linear transmittance; α_0: linear absorption coefficient; β_{eff}: nonlinear coefficient; Im $\chi^{(3)}$: imaginary third-order susceptibility

Laser	Input pulse energy	Sample	T_0 (%)	α_0 (cm^{-1})	β_{eff} (cm GW^{-1})	Im $\chi^{(3)}$ ($\times 10^{-12}$, esu)
532 nm	250 μJ, 10 Hz	CP in DMF	81.66	2.03	—	—
		Annealed CP in DMF	80.03	2.23	−1.22	−0.42
	250 μJ, 2 Hz	3% CP/PMMA	45.99	221.93	226.95	96.99
		3% annealed CP/PMMA	54.10	122.87	242.67	103.71
		6% CP/PMMA	23.80	205.07	342.89	146.53
		6% annealed CP/PMMA	35.28	260.46	818.53	249.80
1064 nm	750 μJ, 10 Hz	CP in DMF	89.20	1.14	—	—
		Annealed CP in DMF	87.32	1.36	1.63	0.56
	600 μJ, 2 Hz	3% CP/PMMA	51.51	189.54	9	3.85
		3% annealed CP/PMMA	58.07	108.70	160.75	68.70
		6% CP/PMMA	27.28	185.57	88.19	37.70
		6% annealed CP/PMMA	39.47	232.41	494.34	211.26

Table 2 Damage thresholds of the samples. CP: the $CH_3NH_3PbI_3$:PVK blends

Laser	Input pulse energy	Sample	Damage threshold (J cm^{-2})
532 nm	250 μJ, 10 Hz	CP in DMF	—
		Annealed CP in DMF	—
	900 μJ, 2 Hz	3% CP/PMMA	45.84
	1100 μJ, 2 Hz	3% annealed CP/PMMA	60.79
	900 μJ, 2 Hz	6% CP/PMMA	39.30
	1000 μJ, 2 Hz	6% annealed CP/PMMA	48.19
1064 nm	750 μJ, 10 Hz	CP in DMF	—
		Annealed CP in DMF	—
	2000 μJ, 2 Hz	3% CP/PMMA	37.87
	2200 μJ, 2 Hz	3% annealed CP/PMMA	43.76
	1800 μJ, 2 Hz	6% CP/PMMA	32.48
	2000 μJ, 2 Hz	6% annealed CP/PMMA	36.09

 This journal is © The Royal Society of Chemistry 2017

Open Access Article. Published on 12 January 2017. Downloaded on 11/7/2025 3:24:31 PM.
This article is licensed under a Creative Commons Attribution 3.0 Unported Licence.

To quantitatively compare the NLO characteristics of these samples, the Z-scan data were numerically fitted by using the nonlinear absorption model in the literature.[21] The β_{eff} value as a function of the excitation pulse energy are depicted in Fig. 4c and d. As we can see, the β_{eff} coefficients of all the samples rise steadily as the energy clamping at both 532 and 1064 nm. In contrast to the non-annealed films and the annealed film with lower CP concentration, the annealed film with higher CP concentration has a larger coefficient and superior OL performance, as summarized in Table 1. The nonlinear extinction coefficients reported in this work are much larger than those shown in some graphene, GO, PcZn and GO–PcZn samples.[22–24] These advantages make the annealed CP-doped PMMA films to be potential candidates for broadband optical limiters in both the visible and near-infrared regimes. Table 2 gives the damage thresholds of these blends at different laser input energies.

Conclusions

The NLO and OL properties of the CP blends, which were dispersed in DMF and embedded as inclusions in a PMMA matrix, respectively, were experimentally studied by open aperture Z-scan method. In contrast to the non-annealed CP dispersed in DMF, which showed no NLO response at both 532 and 1064 nm, the annealed blends exhibited a SA response at 532 nm in the same DMF solution. At 1064 nm, the annealed sample displayed different NLO responses: SA at the lowest pulse energy of 250 μJ and RSA at the higher pulse energy of more than 350 μJ. When these blends were embedded into a commercially available polymer PMMA, all the CP-doped PMMA films showed RSA response, much larger nonlinear absorption coefficient and more superior OL performance when compared to the same blends in solution.

Acknowledgements

This work is supported by the National Natural Science Foundation of China (61378072, 61522510, 61675217), Joint project of Ministry of Education and State Administration of Foreign Experts Affairs (TS2010HDLG024) and the External Cooperation Program of BIC, CAS (181231KYSB20130007), the "Strategic Priority Research Program" of CAS (XDB16030700), and the Key Research Program of Frontier Science, CAS (QYZDB-SSW-JSC041). We also acknowledge Prof. Werner J. Blau at Trinity College Dublin for his helpful discussion in this work.

Notes and references

1 Y. Chen, J. Wang, N. He, W. J. Blau, M. Feng, H. Zhan, B. Zhang, J. H. Zhu, L. J. Niu and P. P. Li, Nanomaterials for optical limiting, in *Encyclopedia of Nanoscience and Nanotechnology*, ed. H. S. Nalwa, American Scientific Publishers, California, 2011, vol. 18, p. 45.
2 Y. Chen, T. Bai, N. Dong, F. Fan, S. Zhang, X. Zhuang, J. Sun, B. Zhang, X. Zhang, J. Wang and W. J. Blau, *Prog. Mater. Sci.*, 2016, **84**, 118.
3 Y. Chen, M. Hanack, Y. Araki and O. Ito, *Chem. Soc. Rev.*, 2005, **34**, 517.
4 Y. Chen, M. E. EI-Khouly, J. J. Doyle, Y. Lin, Y. Liu, E. Notaras, W. J. Blau and S. M. O'Flaherty, Phthalocyanines and related compounds: nonlinear optical response and photoinduced electron transfer process, in *Handbook of Organic Electronics and Photonics*, ed. S. Ranch, USA California, American Scientific Publishers, 2008, pp. 151–181.
5 J. Wang, Y. Chen and W. J. Blau, *J. Mater. Chem.*, 2009, **19**, 7425.
6 F. D. Angelis, *Acc. Chem. Res.*, 2014, **47**, 3349.
7 W. Wang, M. O. Tadé and Z. Shao, *Chem. Soc. Rev.*, 2015, **44**, 5371.
8 H. S. Jung and N. G. Park, *Small*, 2015, **11**, 10.
9 S. Shi, Y. Li, X. Li and H. Wang, *Mater. Horiz.*, 2015, **2**, 378.
10 C. C. Stoumpos, C. D. Malliakas and M. G. Kanatzidis, *Inorg. Chem.*, 2013, **52**, 9019.
11 G. Xing, N. Mathews, S. Sun, S. S. Lim, Y. M. Lam, M. Grätzel, S. Mhaisalkar and T. C. Sum, *Science*, 2013, **342**, 344.
12 S. D. Stranks, G. E. Eperon, G. Grancini, C. Menelaou, M. J. P. Alcocer, T. Leijtens, L. M. Herz, A. Petrozza and H. J. Snaith, *Science*, 2013, **342**, 341.
13 F. Hao, C. C. Stoumpos, R. P. H. Chang and M. G. Kanatzidis, *J. Am. Chem. Soc.*, 2014, **136**, 8094.
14 H. S. Kim, C. R. Lee, J. H. Im, K. B. Lee, T. Moehl, A. Marchioro, S. J. Moon, R. Humphry-Baker, J. H. Yum, J. E. Moser, M. Grätzel and N. G. Park, *Sci. Rep.*, 2012, **2**, 591.
15 C. A. Walsh and D. M. Burland, *Chem. Phys. Lett.*, 1992, **195**, 309.
16 Y. Zhang, T. Wada and H. Sasabe, *J. Mater. Chem.*, 1998, **8**, 809.
17 J. V. Grazulevivius, P. Strohrirgl, J. Pielichowski and K. Pielichowski, *Prog. Polym. Sci.*, 2003, **28**, 1297.
18 Y. A. Berlin, F. C. Grozema, L. D. A. Siebbeles and M. A. Ratner, *J. Phys. Chem. C*, 2008, **112**, 10988.
19 L. L. Wang, C. McCleese, A. Kovalsky, Y. X. Zhao and C. Burda, *J. Am. Chem. Soc.*, 2014, **136**, 12205.
20 Y. M. Xiao, G. Y. Han, Y. Z. Chang, Y. Zhang, Y. P. Li and M. Y. Li, *J. Power Sources*, 2015, **286**, 118.
21 K. Wang, J. Wang, J. Fan, M. Lotya, A. O'Neill, D. Fox, Y. Feng, X. Zhang, B. Jiang, Q. Zhao, H. Zhang, J. N. Coleman, L. Zhang and W. J. Blau, *ASC Nano*, 2013, **7**, 9260.
22 X. Cheng, N. Dong, B. Li, X. Zhang, S. Zhang, J. Jiao, W. J. Blau, L. Zhang and J. Wang, *Opt. Express*, 2013, **21**, 16486.
23 Z. B. Liu, Y. Wang, X. L. Zhang, Y. F. Xu, Y. S. Chen and J. G. Tian, *Appl. Phys. Lett.*, 2009, **94**, 021902.
24 J. H. Zhu, Y. X. Li, Y. Chen, J. Wang, B. Zhang, J. J. Zhang and W. J. Blau, *Carbon*, 2011, **49**, 1900.